

Study of Biomechanical Response of Human Hand-Arm to Random Vibrations of Steering Wheel of Tractor

G. Geethanjali* and C. Sujatha†

Abstract: This paper reports a study on the biomechanical response of a human hand-arm model to random vibrations of the steering wheel of a tractor. An anatomically accurate bone-only hand-arm model from TurboSquidTM was used to obtain a finite element (FE) model to understand the Hand-arm vibration syndrome (HAVS), which is a neurological and vascular disorder caused by exposure of the human hand-arm to prolonged vibrations.

Modal analysis has been done to find out the first few natural frequencies and mode shapes of the system. Coupling of degrees of freedom (DOF) had to be done in the FE idealization to do modal analysis, as the bones were not attached to each other in the TurboSquidTM model. The shoulder bone, scapula, has been constrained at one end for eigenvalue analysis. It was observed that the first five natural frequencies were in the range of 0-250 Hz, which is the range in which the effect of HAVS is the highest. Harmonic analysis was done by giving a swept sine excitation in the frequency range 0 to 200 Hz. For this, a force input of 25 N was imparted at nodes perpendicular to the hand, the force value chosen being the nominal force in most applications involving powered hand-held tools and steering wheels of tractors. The nodes chosen for force application were determined experimentally from observations made by gripping the steering wheel. The frequency response function (FRF) plots were obtained in the x, y and z directions.

Random vibration analysis was done next by giving force power spectral densities (PSD) in the form of nodal excitation as input to the FE model of hand-arm, and computing the output acceleration PSDs. The input force PSDs were measured using FlexiForce[®] sensors along the three axes. The acceleration responses at the steering wheel were also measured using tri-axial accelerometers for validating the computed results. The output acceleration PSDs were then weighted using the frequency weighting curves for hand-arm vibration and the total daily exposure A(8), computed using ISO 5349-1 standards, was compared with the vibration action and

* Student, IIT Madras, Chennai, India.

† Professor, IIT Madras, Chennai, India.

limit values. The A(8) values obtained are found to be higher than the vibration limit values.

Keywords: Hand-arm vibration syndrome, finite element modeling, hand-transmitted vibrations, daily vibration exposure value.

1 Introduction

Hand-arm vibrations are vibrations transmitted to hand and arms due to the use of powered hand-held tools like power drills, chainsaws, pneumatic drills, etc., and steering wheels of heavy vehicles. Operators of such tools and vehicles are exposed to high levels of vibration, mostly in the frequency range 10-500 Hz. Long term exposure to such vibrations causes Hand-arm vibration syndrome, which is a complex disease with sensorineural, vascular and musculoskeletal deficits. It is mainly a neurological and vascular disorder. Neurological features include numbness, tingling sensation and pain and the vascular features are blanching of fingers. Minor damages to muscles, bones and joints may also occur with the sufferer losing fingers in extreme cases. Also, with further vibration exposure, nutritional changes may occur to the finger pulps leading to the formation of small areas of skin necrosis at finger tips as reported by Gurram *et al.* (1995).

These severe health risks have prompted the study of the vibration response characteristics of the human hand-arm in the present paper. The hand-arm system is a highly complex non-homogeneous continuous system comprising visco-elastic properties of muscles, bones, skin, etc. In order to know more about the causes and effects of these hand-arm vibrations, the hand and arm have been thoroughly studied. The present study deals with an anatomically accurate hand-arm bone-only model from TurboSquidTM designed by doctors using the human anatomy and their clinical knowledge. This model is idealized using finite elements for the purpose of calculation of the daily exposure value A(8) of the vibrations induced by the steering wheel of a tractor.

2 About hand-arm bones

The human hand-arm system is highly complex and continuous. It comprises 31 bones, beginning from the hand to the shoulder bone. They are: scapula, the shoulder blade; humerus, the upper arm bone; radius and ulna; the forearm bones; carpals (8 bones); metacarpals (5 bones) and the phalanges (14 bones), which make up the hand and wrist. The carpal bones are arranged in two rows and are named based on their shapes. The five metacarpal bones are cylindrical in shape and meet the distal carpals at one end and the phalanges at the other end. These metacarpal bones

form the palm. The fingers consist of the phalanges. There are three phalanges for each finger and two for the thumb, making their number 14 as described by Freivalds (2004). The radius and ulna are responsible for the motion of the hand, i.e., pronation and supination from the neutral position. The radius rotates about the ulna, which is the larger and longer of the two bones. The bone of the upper arm, called the humerus, is the largest and the longest bone in the arm. The elbow joint is formed by the articulations between three bones: the radius, the humerus and the ulna.

3 Finite element (FE) modelling

The present study to comprehend HAVS has been conducted on a 3 dimensional (3-D) FE model with an elbow angle of 90° in ANSYS. The scope of the work covers only this geometry of the hand-arm system, considering that the driver/operator grips the steering wheel/ power tool in this position (Cherian *et al.*, 1996). In reality, the elbow angle is actually dynamic (continuously changing geometry), being driver/operator dependent and might be greater than 90° , leading to minor variations in the results.

An anatomically accurate hand-arm bone-only model from TurboSquidTM has been used for this purpose. The arm which was in fully extended state in the original TurboSquidTM model was brought to neutral position (90° angle at the elbow joint) as shown in Fig. 1 using an animation software called Autodesk 3DS Max (2012). In the original model, attention had been given to accurate modelling of the anatomical details of each bone, e.g., margins, surfaces, tuberosities, grooves and all other important anatomical landmarks, resulting in a very large number of faces. Autodesk 3DS Max was used to reduce the number of faces of the bones to 20 percent of the initial number for reduction of computational time and effort. The element type chosen was Solid 187, which is a 10 node tetrahedral element, used for modeling irregular meshes and which gives more accurate results as compared to Solid 72, a 4 node tetrahedral element (ANSYS, 2009).

The bone is an orthotropic material and its properties have been obtained for a 30 year old man of height 1.7 m and weight 70 kg from the paper by Rodríguez *et al.* (2006) as shown in Table 1. With increase in age, the bones tend to become brittle and hence the results might vary for different people. Also, a bone-only model has been considered for the study. Damping of 12% was used for this computation based on the value reported by Tsuchikane *et al.* (1995) for studies done on the human leg. The paper states that the minimum damping ratio for the tibia of the leg is 2 % for the case where only the bones are considered and the maximum damping ratio is 19 % with the skin, muscles, ligaments, tendons and tissues considered. The leg, as is known, has more muscle and skin than the hand. So the damping

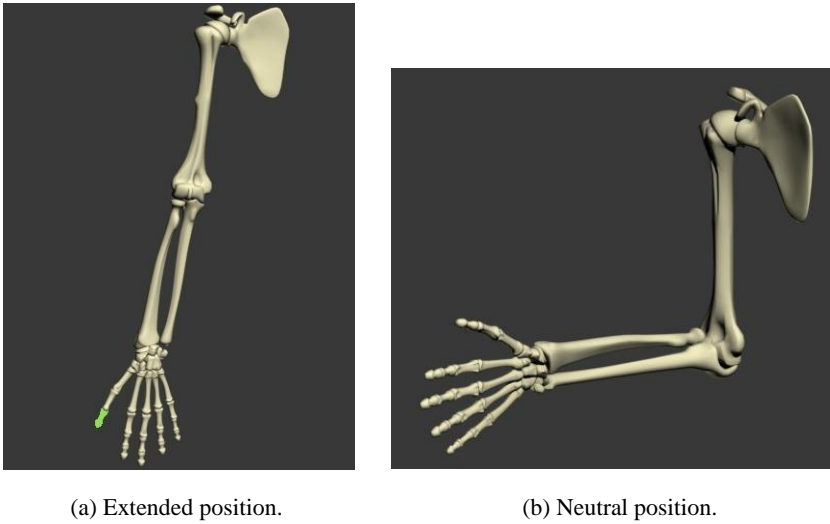


Figure 1: Hand-arm model.

of the hand has been assumed to be 12% in the present work with muscles, skin, ligaments, tendons and tissues included. The actual damping values change from person to person and these could affect the results. With changes in age and gender, the material properties and hence the results will change, but this study is not within the scope of this paper.

Table 1: Properties of bone (Rodriguez, Julio, and Arroyo (2006)).

Property	Units	Property	Units
E_x	6910 N/mm ²	ν_{zx}	0.22
E_y	8510 N/mm ²	G_{xy}	2410 N/mm ²
E_z	18400 N/mm ²	G_{yz}	4910 N/mm ²
ν_{xy}	0.38	G_{zx}	3560 N/mm ²
ν_{yz}	0.24	ρ	1500 kg/m ³

Coupling of degrees of freedom (DOFs) was done to overcome the problem of bones being unconnected with each other in the original bone-only hand-arm TurboSquidTM model due to the absence of ligaments, muscles and tendons. To achieve this, an option called Couple DOF was used, making it possible to force a set of nodes to have the same DOF. Every node on every end of a bone was indi-

vidually attached to every node on the adjacent bone's end. This was a very time consuming process as 31 bones had to be attached to each other in all possible ways. Figs. 2 and 3 show the hand bones without coupling and with coupling. The shoulder bone, scapula was then constrained at one end, partially, as a displacement constraint. The complete model with constraints and coupling has been shown in Fig. 4.

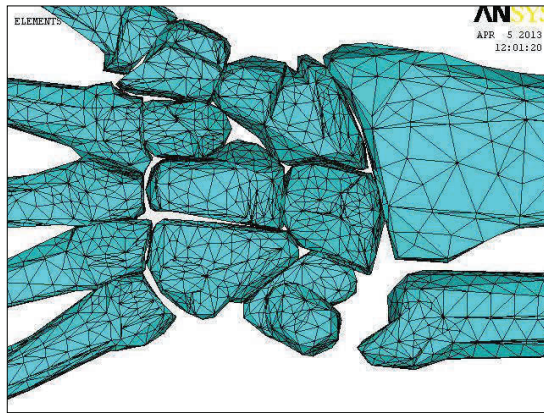


Figure 2: Hand bones without coupling.

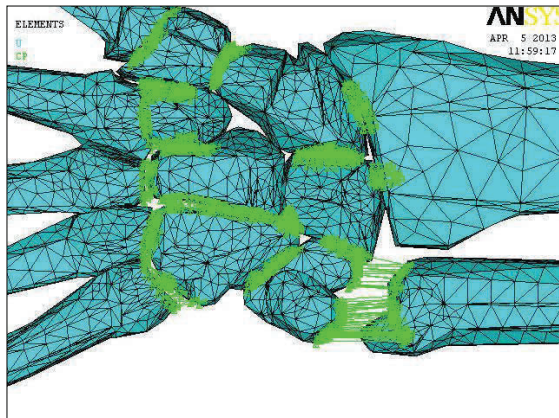


Figure 3: Hand bones with coupling.

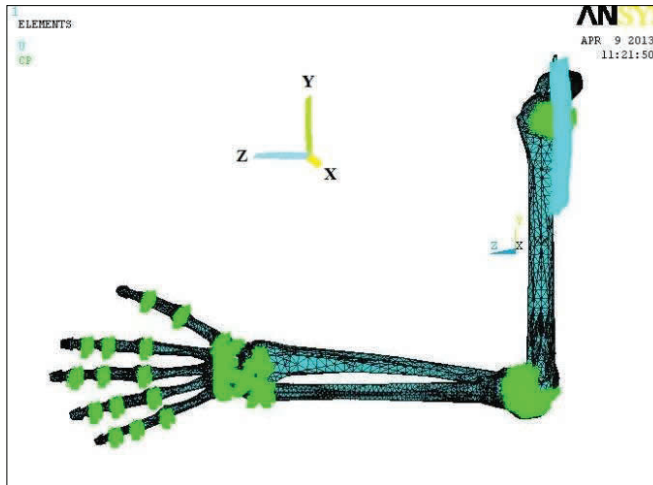


Figure 4: FE model with constraints and coupling.

4 Modal analysis

Modal analysis has been done to extract the first few modes and the first five natural frequencies, which have the maximum influence on hand-arm dynamics, have been listed in Table 2, along with a description of the mode shapes. It has also been reported by Cherian *et al.* (1996) that HAVS has its maximum effect in the frequency range 10-200 Hz. It has been observed from the paper by Lundstrom (1984) that the natural frequency of the palm is around 80 Hz and this is quite close to the second natural frequency (71.89 Hz) of the hand-arm system being studied. Hence this mode has been identified to be the one having the maximum effect on HAVS. The deformed shape with undeformed edge has been shown for the second mode at 71.89 Hz in Fig. 5.

5 Harmonic analysis

Harmonic analysis is the process of giving a swept sine excitation to a system to study its response. In the present hand-arm model, partial constraining of the scapula was given in the form of a displacement constraint. A force of 25 N was decided upon from literature as the nominal value of grip force in applications involving use of steering wheels of tractors. Also, the force does not actually act as a point load. Hence, the nodes on which the force acts were determined by gripping the steering wheel manually to find approximately the region of the hand directly exposed to the force and 311 nodes were identified as shown in Fig. 6. The force

Table 2: Natural frequencies and mode shapes.

Mode	Natural frequency (Hz)	Mode shape
1	41.86	Longitudinal motion (z) of hand, forearm and upper arm
2	71.89	Rotation of hand, forearm & upper arm about longitudinal (z) axis through shoulder joint
3	91.24	Rotation of hand and forearm about lateral (x) axis through elbow joint
4	158.9	Rotation of upper arm about lateral (x) axis through elbow joint
5	181.06	Rotation of hand, forearm and upper arm about vertical (y) axis through shoulder joint

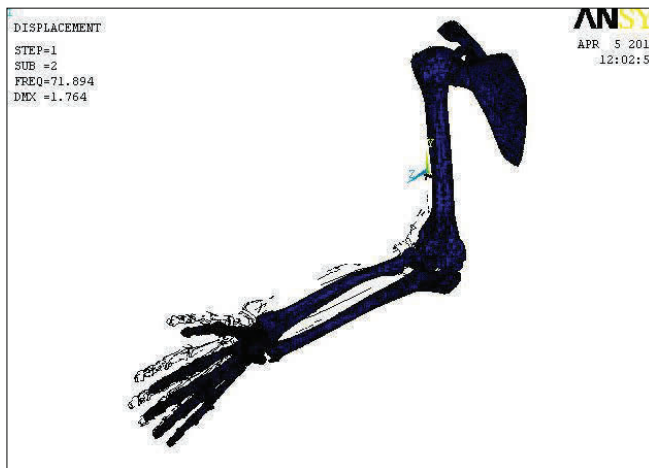


Figure 5: Deformed shape with undeformed edge of mode 2.

of 25 N was applied as a distributed load over these nodes in a direction perpendicular to the hand. Stepped sine excitation was given in the frequency range of 0-200 Hz to obtain the FRF plots. The results of this analysis are the FRF plots in the x, y and z directions with the frequency axis depicted in the linear scale and the displacement magnitude shown on a logarithmic scale. They have been shown in Figs. 7-9. With the force given in the x direction, it can be observed that the predominant response is that of the 2nd natural frequency, irrespective of whether

the response is along the x, y or z directions.

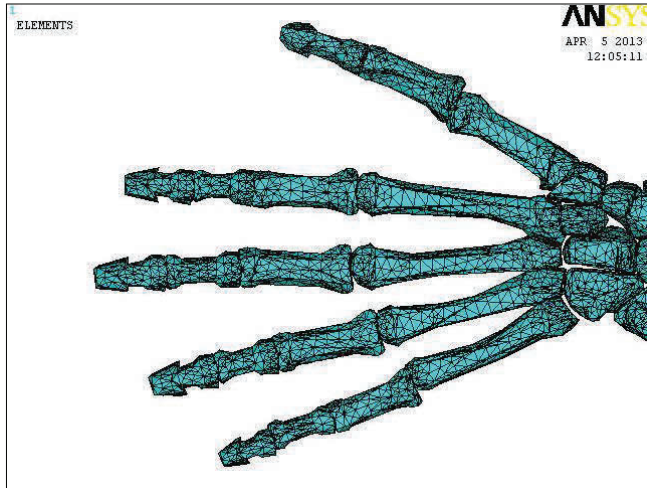


Figure 6: Grip nodes of the hand.

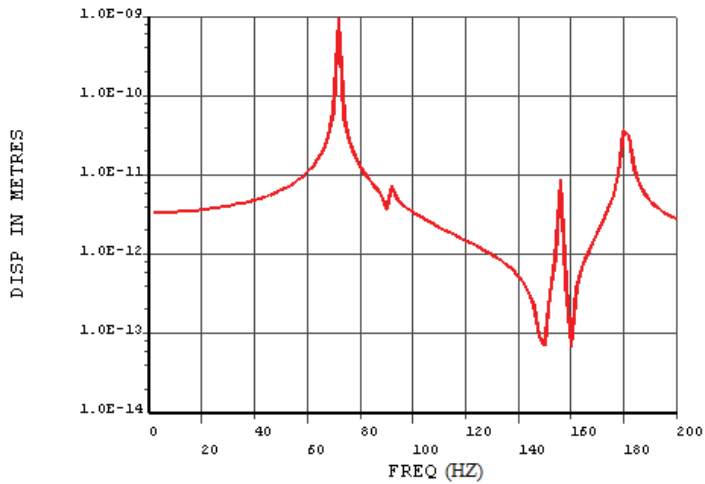


Figure 7: FRF plot: Force in x-direction, response in x-direction.

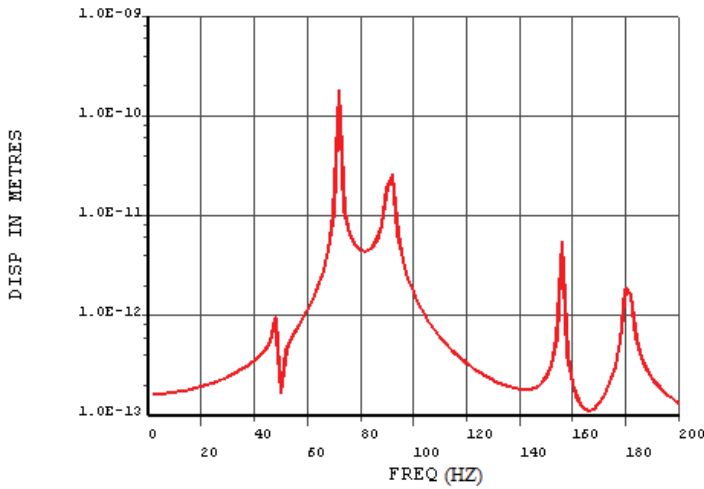


Figure 8: FRF plot: Force in x-direction, response in y-direction.

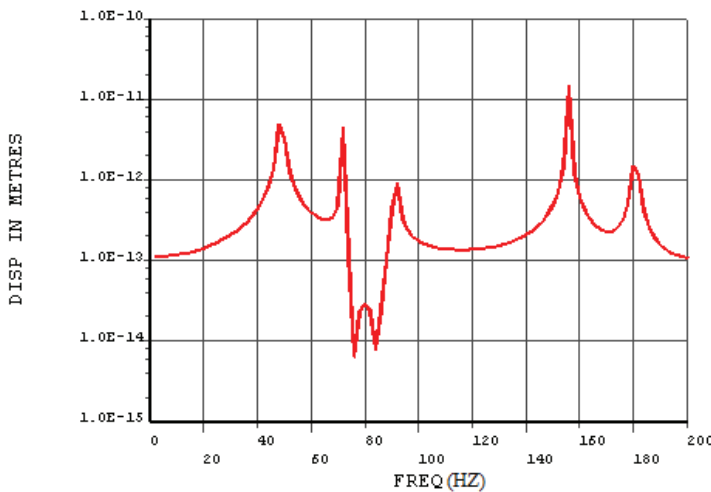


Figure 9: FRF plot: Force in x-direction, response in z-direction.

6 Measurement of forces at the steering wheel of tractor

A two-wheel drive tractor, Mahindra Sarpanch 475 DI, with a power of 42 HP was chosen for the measurement. The forces at the steering wheel were measured using FlexiForce® sensors. B201 sensors (Fig. 10) with a force rating of 0-667 N (Medium) were chosen for measuring the forces; these sensors have the capabil-

ity to measure both static and dynamic loads. The sensors were conditioned and calibrated before their usage, the calibration curve being as shown in Fig. 11.



Figure 10: B201 FlexiForce® sensor.

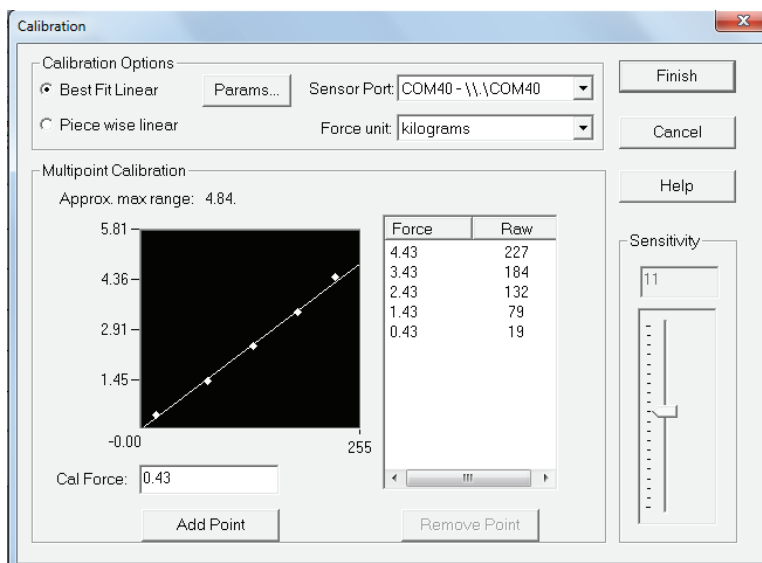


Figure 11: Calibration window.

A fixture (Fig. 12), made of acrylic material, facilitated the use of 2 FlexiForce® sensors at a time on each hand on the steering wheel. This fixture also ensured that the forces were transmitted uniformly and only in the direction normal to the sensors. These 4 sensors fitted into the sensor handles were connected to the Multi handle economic load and force (MELF) system. The MELF software ensured that the forces were directly recorded on a laptop as time histories as shown in Fig. 13. The maximum sampling frequency possible for this equipment was 200 Hz. This

was a limitation and so the maximum frequency up to which a proper response could be expected was reduced to 80 Hz. The second natural frequency of the hand that occurs at 71.9 Hz (and which has the maximum effect) is within this range. All the measurements were made on a relatively smooth road in the second gear in no load condition.



Figure 12: Fixture with sensor.

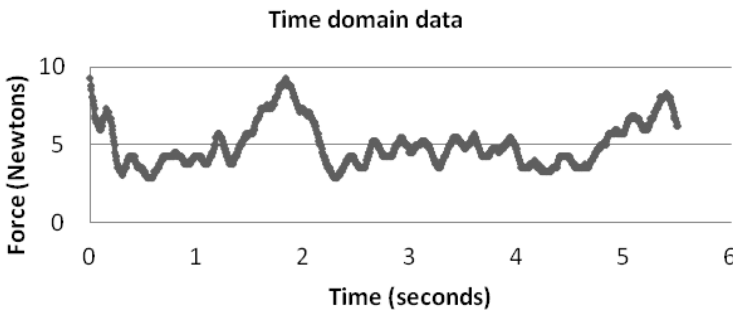


Figure 13: Force data in time domain.

7 Random vibration analysis and calculation of daily exposure A(8) from measured force PSDs

The data from the MELF system recorded in time domain was converted to frequency domain using MATLAB (2010). This force PSD obtained from MATLAB (Fig. 14) was then given as nodal excitation to points on the fingers of the ANSYS hand-arm model. Damping of 12% was used for this computation based on the value reported by Tsuchikane *et al.* (1995) as explained before. The output PSD

obtained from ANSYS as a narrow-band spectral density had to be converted to 1/3rd octave bands for it to be weighted using the frequency weighting curves of hand-arm vibration (HAV) according to ISO 5349-1 (2001) as shown in Fig. 15.

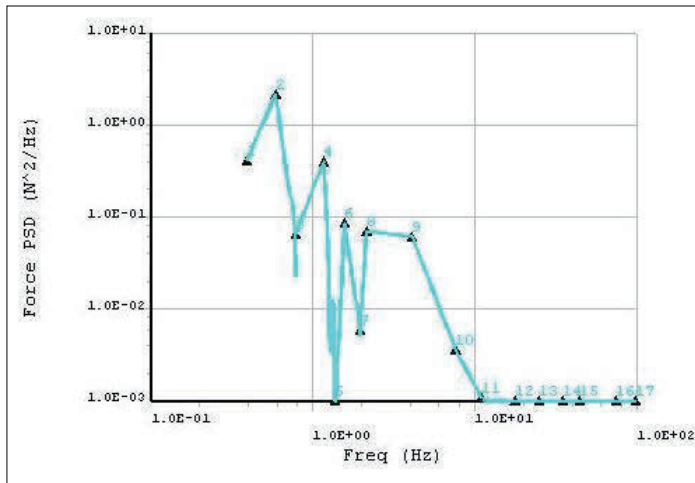


Figure 14: Input force PSD.

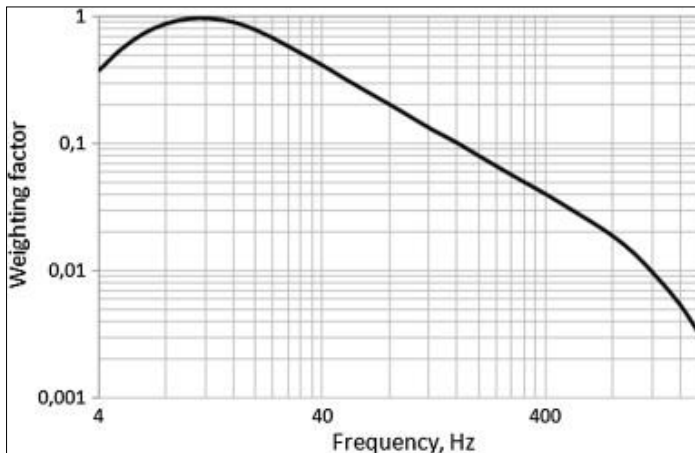


Figure 15: Frequency weighting curve for HAV.

The output acceleration PSD was used to calculate the frequency weighted accelerations a_{hw_x} , a_{hw_y} and a_{hw_z} in three directions x, y and z, using MATLAB and ISO

5349-1 weighting curves. The frequency weighted acceleration a_{hw} was computed as

$$a_{hw} = \left[\sum_{j=1}^n (W_j a_{wj})^2 \right]^{1/2} \quad (1)$$

where W_j is the weighting factor and a_{wj} is the measured acceleration in m/s^2 in the j^{th} one third octave band.

The total vibration value a_{hv} was calculated using Eq. (2)

$$a_{hv} = \sqrt{a_{wx}^2 + a_{wy}^2 + a_{wz}^2} \quad (2)$$

Daily exposure A(8) was calculated for a daily exposure of 4 hours using Eq. (3) below.

$$A(8) = a_{hv} \sqrt{\frac{T}{T_0}} \quad (3)$$

where T is the exposure time in hours and T_0 is the reference duration of 8 hours. Table 3 shows the accelerations computed for obtaining A(8).

Table 3: Computation of daily exposure

Parameter	Value
Weighted acceleration a_{hw_x} (m/s^2)	12.77
Weighted acceleration a_{hw_y} (m/s^2)	0.0189
Weighted acceleration a_{hw_z} (m/s^2)	0.0073
Total vibration value a_{hv} (m/s^2)	12.77
Daily exposure A(8) (m/s^2)	9.03

8 Measurement of A(8) using human vibration meter

The analytically obtained A(8) value calculated from the output acceleration PSD of the FE model was validated using measurements. For this a Human vibration meter VM30-H with a tri-axial accelerometer measuring the acceleration values simultaneously in all the three directions was used to measure the total acceleration value (A_{hv}). A mounting accessory was used to fix the accelerometer to the steering wheel (Fig. 16). The output A_{hv} of VM30-H tri-axial accelerometer was fed into the A(8) calculator, to compute the A(8) value for a duration of 4 hour usage in an 8



Figure 16: Tri-axial accelerometer with handle.

Table 4: Comparison of daily exposure: Analysis and experiment

Parameter	Value
Daily exposure A(8) from analysis	9.03 m/s ²
Daily exposure A(8) from measurement	10.6 m/s ²
EU Vibration exposure action value	2.5 m/s ²
EU Vibration exposure limit value	5 m/s ²

hour day. Table 4 shows a comparison of daily exposure obtained from experiment and calculation and the match is good.

The values obtained are clearly higher than the exposure action and limit values of 2.5 m/s² and 5 m/s² respectively, as specified by European Union Physical Agents Directive (Vibration). These high values can be attributed to the excessive vibrations emanating from the steering wheel.

9 Conclusions

An accurate bone-only FE model of the human hand and arm has been made for understanding HAVS better and finding out the daily exposure value A(8). The values were obtained by two methods: (i) computing A(8) by feeding experimentally measured force PSDs as input to an FE model of the hand-arm system and (ii) using tri-axial accelerometers for measurement. There is a good correlation between the two. The results show that the A(8) values obtained are much higher than the exposure action and limit values. It can be inferred from this that tractor drivers are prone to HAVS in the long run. Hence measures like use of anti-vibration gloves, altering work practices and the way work is organised to reduce exposure to vibration, maintaining equipment, etc., have to be undertaken to reduce the risk of contracting HAVS.

References

1. ANSYS (2009) 12.1 Version, Analysis.
2. AUTODESK 3DS MAX, (2012) 3-D Modelling and Animation Software.
3. Cherian, T., Rakheja, S., Bhat, R. B. (1996) An Analytical Investigation of an Energy Flow Divider to Attenuate Hand Transmitted Vibration. *International Journal of Industrial Ergonomics*, 17, 455-467.
4. Freivalds, A. (2004) *Biomechanics of the Upper Limbs- Mechanics, Modelling and Musculoskeletal Injuries*. CRC Press.
5. Gurram, R., Rakheja, S., Gouw, G. J. (1995) Mechanical impedance of the human hand arm system subject to sinusoidal and stochastic excitations. *International Journal of Industrial Ergonomics*, 16, 135-145.
6. International Organization for Standardization, ISO 5349-1:2001. *Mechanical Vibration and Shock-Measurement and Evaluation of Human Exposure to Hand-Transmitted Vibration, Part 1: General Requirements*, ISO, Switzerland.
7. Lundstrom, R. (1984) Local vibrations-Mechanical impedance of the human hand's glabrous skin. *Journal of Biomechanics*, 17, 2, 137-144.
8. MATLAB (R2010a) Mathematical Computing Software
9. Rodríguez, G. B., Julio, S., Arroyo, R. L. (2006) Simulation nonlinear biomechanics of the forearm, using ANSYS. *Proceedings of International ANSYS Conference: A World Simulation*, Pittsburgh PA, USA
10. Tsuchikane, A., Nakatsuchi, Y., Nomura, A. (1995) The influence of joints and soft tissue on the natural frequency of the human tibia using the impulse response method. *Proceedings of the Institution of Mechanical Engineers, Part H: Journal of Engineering in Medicine*, 209, 149-155.
11. TurboSquid, URL <http://www.turbosquid.com>

